JVSTB Journal of Vacuum Science & Technology B

# Accurate resonant frequency spacing of microring filters without postfabrication trimming

C. W. Holzwarth, T. Barwicz, M. A. Popovi, P. T. Rakich, E. P. Ippen, F. X. Kärtner, and Henry I. Smith

Citation: Journal of Vacuum Science & Technology B **24**, 3244 (2006); doi: 10.1116/1.2363402
View online: http://dx.doi.org/10.1116/1.2363402
View Table of Contents: http://scitation.aip.org/content/avs/journal/jvstb/24/6?ver=pdfcov
Published by the AVS: Science & Technology of Materials, Interfaces, and Processing

# Accurate resonant frequency spacing of microring filters without postfabrication trimming

C. W. Holzwarth,[a] T. Barwicz, M. A. Popović, P. T. Rakich, E. P. Ippen, F. X. Kärtner, and Henry I. Smith
*Research Laboratory of Electronics, Massachusetts Institute of Technology Cambridge, Massachusetts 02139*

(Received 6 August 2005; accepted 18 September 2006; published 4 December 2006)

Optical microring resonators are compact building blocks for many microphotonic systems, as they enable narrow-band filtering. Of particular interest are integrated banks of microphotonic filters, with accurately spaced operational frequencies, for simultaneously processing multiple channels of information. Accurate spectral spacing has not yet been reported as it requires subnanometer control of the average dimensions of the optical resonators used to build high-performance microphotonic filters. Here, the authors present a technique enabling the relative dimensional control needed to achieve accurate spectral spacing, without postfabrication trimming. The authors fabricated eight-channel second-order microring-resonator filter banks with accurate spectral spacing using scanning-electron-beam lithography. The microrings are made of silicon-rich silicon nitride, and the subnanometer relative dimensional control is achieved through carefully calibrated adjustments of the electron-beam dose. When combining the dose alternations with small changes in microring radii, the authors demonstrate filter banks with accurate channel spacings ranging from 90 to 180 GHz. We show that we can accurately control a 2.7 nm change in average width of the ring waveguide to 0.11 nm, despite a 6 nm step size in the scanning-electron-beam lithography system. © *2006 American Vacuum Society.* [DOI: 10.1116/1.2363402]

## I. INTRODUCTION

Microring-resonator-based filters are an essential part of many proposed microphotonic systems from optical add-drop multiplexers to photonic analog-to-digital converters. Recent progress in design and fabrication of high-index-contrast (HIC) microring resonators has made possible the low loss and wide spectral spacing between resonances required for real-world applications.[1] Achieving accurate resonant frequency spacing of microring filters is critical for many of these applications, but this has not yet been demonstrated without postfabrication trimming. In this article, we present a fabrication technique, using scanning-electron-beam lithography (SEBL), that enables the accurate control of the resonant frequency spacing of HIC microring-resonator filter banks.

Resonant frequency control in microring-resonator filters is achieved by controlling the optical path length of a ring, which depends on the ring's radius and the phase velocity of light in the ring. (The resonant frequency condition corresponds to there being an integral number of wavelengths around the ring.) The phase velocity depends on the width of the ring waveguide. The level of frequency control needed in proposed optical systems is very application specific but is typically on the order of 1 GHz or better. To achieve this level of frequency control one must control the average width of the ring waveguide to within 10–50 pm, where the exact number depends on the ring waveguide cross section and index contrast. This is about 100 times finer than the minimum step size of the address grid of an SEBL system; therefore, to achieve this kind of width control, we adjusted the electron-beam dose.[2]

In this study, second-order (i.e., two rings) microring-resonator filters with 20 nm free-spectral range, 50 GHz bandwidth and $1.5 \pm 0.5$ dB drop loss were fabricated in silicon-rich silicon nitride (SiN) (refractive index, $n=2.18$ at 1550 nm). Calibration experiments were performed to find the filter's resonant frequency dependency on lithographic parameters such as the specified radius, width, and exposure dose. This information was used to fabricate eight-channel microring-resonator filter banks with accurate resonant-frequency spacing ranging from 90 to 180 GHz. The experimental results show that we can accurately control a 2.7 nm change in average width of the ring waveguide to within 0.11 nm, despite a 6 nm SEBL address grid spacing.

## II. EXPERIMENT

### A. Filter design

The primary objective of this study was to fabricate an eight-channel microring-resonator filter bank with accurate channel spacing for an integrated electronic-photonic analog-to-digital converter, described in detail elsewhere.[3] Specifications included a 20 nm spectral spacing between resonances and a 3 dB bandwidth of 50 GHz. The filter passband requires a sharp roll-off so that there is less than 30 dB crosstalk between adjacent channels spaced at 150 GHz. Furthermore, the power lost in the filter must be less than 3 dB. For this, the second-order microring-resonator design shown in Fig. 1 met all of these specifications, without the need to

[a]Electronic mail: cwh@mit.edu

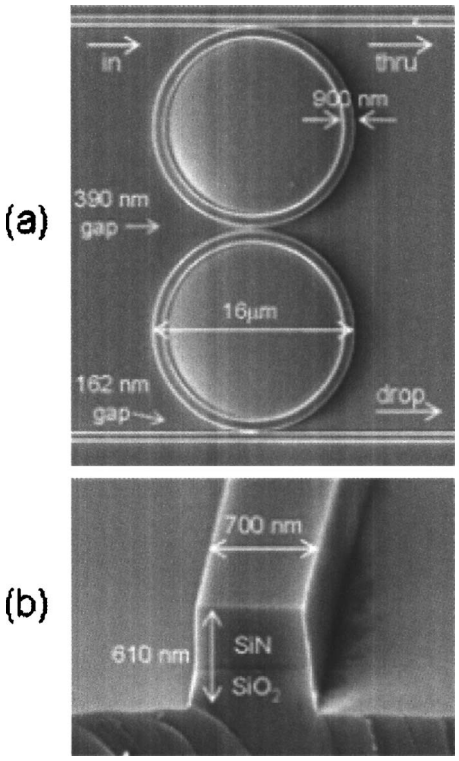


FIG. 1. (a) Scanning-electron micrographs of second-order microring-resonator filter with the designed filter dimensions labeled. Actual fabricated dimensions vary from design by 5 nm or less. (b) Cross section view of bus waveguide etched into 400 nm of SiN and 210 nm of $SiO_2$.

correct for any frequency mismatch due to coupling induced frequency shifts or proximity effects that occur in higher-order microring filters.[4]

### B. Frequency calibration

Simulations were performed using a two-dimensional cylindrical mode solver to calculate the dependence of the ring's resonance frequency on the inner and outer ring radius and the ring waveguide cross section. These simulations showed that a 1 nm increase in ring radius and waveguide width would produce resonant frequency shifts of −18.4 and −33 GHz, respectively. This high sensitivity to dimensional changes, combined with the discrete 6 nm address grid of the SEBL system, limits the channel spacing possible though changes in the pattern layout to linear combinations of −110 and −198 GHz shifts. To overcome this limitation and fabricate the desired filter bank with channels spaced 150 GHz apart, we adjusted the electron-beam dose used and achieved control of waveguide width on a scale of tens of picometers

Dose modulation has been used previously to correct for the resonant frequency mismatch in third-order microring-resonator filters.[5] It is well known that when used to expose resist on a solid substrate, the point-spread function of a focused electron beam has smoothly sloped edges. This enables one to adjust the width of a written line by adjusting the dose via the dwell time per address point. This change in width remains throughout the fabrication process and in this

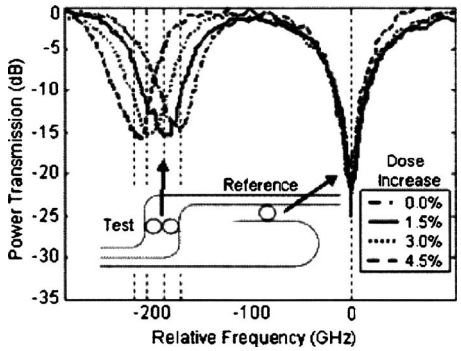


FIG. 2. Sample set of transmission spectra used for dose calibration experiments. Inset displays the device layout with a reference filter for each test filer. All frequencies are measured relative to the reference filter resonant frequency.

study results in a shift in the resonant frequency that is not limited by the address grid step size of the SEBL system.

An empirical calibration was performed to find the resonant frequency's dependence on specified exposure dose, radius, and width. For this it was important to separate frequency shifts due to changes in lithographic parameters from shifts caused by other factors such as slight changes in the SiN thickness and slow drifts of the electron-beam current. To separate these contributions, each calibration test was performed with a reference filter and a test filter located in close proximity to one another. The reference filter was kept unchanged in all cases while the exposure dose, ring widths, and ring radii were varied. The effect of the lithographic alteration on the resonant frequency was determined by measuring the frequency shift of the test filter relative to the resonance frequency of the reference filter (Fig. 2). Since the reference filter and test filter were written consecutively and spaced no more than 100 $\mu$m apart there was not enough distance or write time between them for significant frequency variations due to SiN thickness changes or current drift.

The resonant frequency dependence on changes in specified exposure dose, ring radius, and ring waveguide width are shown and compared with simulated data in Table I. The calibration experiments for radius and width changes are close to the simulated values, whereas the frequency dependency on dose was considerably different, reinforcing the need for empirical calibration. Also, during calibration it was shown that frequency shifts due to changes in dose, radius,

TABLE I. Resonance frequency shift due to specified parameter change.

| Parameter | Optical simulations | Calibration | Filter banks |
|---|---|---|---|
| Radius in *e*-beam layout (GHz/nm) | −18.4 | −17.2±0.9 | −18.0±0.2 |
| Width in *e*-beam layout (GHz/nm) | −33 | −36.6±0.4 | NA |
| Dose (GHz%)[a] | −24 | −12±2 | −11±1 |

[a]Frequency shift due to a 1% change in dose.

and width add linearly within the small range tested. Thus, small modulations in dose can be used to fine tune the discrete, large frequency shifts due to changes in specified radius and width.

The symmetry of the second-order filter suggests that no frequency mismatch should exist between the two microring resonators forming the filter since electron-exposure proximity effects[5] and coupling-induced frequency shifts[4] should affect both resonators similarly. However, a repeatable resonant frequency mismatch between the two resonators forming the filter was observed. By writing the filter at several different locations in the 100 $\mu$m diameter SEBL field, we observed that the frequency mismatch was a function of location. Hence, it is most probably due to intrafield distortions or digital-to-analog converter errors in the SEBL system.[6] This frequency mismatch, once known, can be corrected using dose modulation by writing the two rings in the same filter with slightly different doses.

### C. Filter bank fabrication

Based on the calibration experiments, the changes in exposure dose and ring radius needed to produce eight-channel filter banks with channel spacing ranging from 90 to 180 GHz were calculated and input to the SEBL layout. The filters were all positioned identically in the *e*-beam write field. The frequency mismatch due to intrafield distortion at this location was measured at calibration to be 8 GHz. To correct for this mismatch the average waveguide width of the lower ring in the second-order filters was narrowed by 0.24 nm by reducing its exposure dose by 0.7%.

The fabrication process was similar to that discussed in Ref. 7. The silicon wafer was first thermally oxidized and then a layer of SiN, with a refractive index of 2.18, was deposited by low-pressure chemical-vapor deposition. Next, 200 nm of polymethyl-methacrylate (PMMA), a positive electron-beam resist, and 60 nm of AquaSAVE, a conducting polymer made by Mitsubishi Rayon, were spun onto the wafer. The SEBL step was performed using a Raith 150 system operating at an accelerating voltage of 30 keV. The PMMA was developed and then a 50 nm nickel hard mask was formed using electron-beam evaporation and a lift-off process. The pattern was defined in the SiN using a reactive-ion-etch step that had been optimized for smooth vertical sidewalls. The nickel hard mask was then removed by a chemical etch, and the wafer was cleaved to expose the input and output facets.

### D. Optical measurements

The transmission spectrum of each fabricated device was measured using a tunable laser and InGaAs PIN photodetector coupled to the input and output facets with lensed fibers. Great care was taken to excite only TE polarized modes, resulting in typically 40 dB contrast between polarizations states. Before collecting data both the input and output coupling was maximized using a piezoelectric stage with three degrees of freedom in order to accurately measure the power difference between the drop and thru spectra.

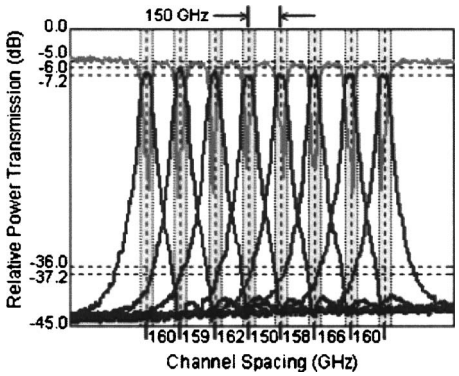


FIG. 3. Measured response of a fabricated eight-channel filter bank with a target channel spacing of 150 GHz. Actual average channel spacing is 158 GHz with less than 30 dB cross talk between adjacent channels.

Transmission measurements for the fabricated filter banks were taken for the common thru port and individual drop ports. Figure 3 shows the transmission spectrum of a fabricated filter bank with a target channel spacing and 3 dB bandwidth of 150 and 50 GHz, respectively. By comparing the drop and thru transmission spectra the drop loss, averaged over 40 filters, was found to be $1.5 \pm 0.5$ dB. The uncertainty of 0.5 dB is attributed to fiber-to-chip coupling loss variations at the input and output facets.

## III. FREQUENCY CONTROL RESULTS

The resonant frequency of the microring filters was found to be controlled within the statistical error of the calibration experiment. The actual channel spacing of the fabricated filters was 4%–5% larger than the targeted spacing. This offset is due to a difference of 0.8 GHz/nm between the resonance frequency dependence on specified radius at calibration and what is seen in the filter banks. This is within the error of the calibration experiment, which is calculated to be 1.0 GHz/nm, for the resonance frequency dependence on specified radius. The calibration of the resonant frequency dependence on dose was found to be even more accurate. The average ring waveguide width change due to dose is measured to be 0.34 nm per 1% change in dose in the filter banks compared to 0.35 nm measured at calibration. This means that the change in average ring waveguide width per percent exposure dose increase varied by only 10 pm between the calibration experiment and the filter bank fabrication. This demonstrates how the technique of dose modulation, after empirical calibration, has the accuracy needed to fabricate filter banks based on HIC microring resonators with channel spacings that are not limited by the SEBL system's discrete address grid.

Dose modulation is also successful in correcting for the resonant frequency mismatch in the second-order filters caused by intrafield distortions. Without dose modulation the filters would have a frequency mismatch of 8 GHz, which is equivalent to an average ring waveguide width difference of 0.24 nm (240 pm) between the two rings. In the fabricated filter banks the frequency mismatch is random in nature with

the best filters having average ring waveguide widths that match within 23 pm. The reason that the average ring waveguide width mismatch is not 23 pm in all filters is due to uncontrollable, but very small, process variations.[2] These process variations result in a standard deviation of the average ring waveguide width of 0.12 nm (120 pm).

The 46.6 GHz bandwidth measured in the individual filters of the filter banks is very close to the designed 50 GHz bandwidth. The bandwidth is mainly determined by the coupling strength between the bus and ring waveguides, which is very sensitive to the filter's dimensions at the coupling region. Therefore, this small difference between the designed and measured bandwidths suggests that the dimensions of the fabricated filters are very close to the design values. Using the Raith 150 SEBL in scanning electron microscopy mode, absolute dimensions of the filters were measured, with 5 nm absolute accuracy, and compared to the targeted dimensions. The ring waveguide, bus waveguide, and bus-to-ring coupling gap widths were measured to be 897, 700, and 166 nm, respectively. All of these measurements are within the 5 nm measurement error to their designed dimensions, demonstrating the high level of absolute dimensional control achieved in the fabricated filters.

The low drop loss of $1.5 \pm 0.5$ dB measured in the filter banks is much better than the system requirement of 3 dB. The major source of this loss is the propagation loss in the ring waveguide. From the radiation quality factor ($Q$) of 53 000, measured in large, weakly coupled rings, the propagation loss is calculated to be 7.7 dB/cm. This propagation loss is mainly due to absorption in the SiN. The SiN absorption loss was measured in an independent experiment employing shallow-etched ridge waveguide structures to be $8 \pm 2$ dB/cm. Accounting for the difference in modal overlap between the ridge waveguides and the rectangular waveguides employed in the filters, the propagation loss expected due to absorption is $6 \pm 2$ dB/cm.

## IV. CONCLUSION

We have discussed fabrication techniques that enable accurate relative control, on the scale of tens of picometers, of the average ring waveguide width of microring-resonator filters. This enabled the fabrication of the first microring-filter banks with accurate resonant frequency spacing, obtained without postfabrication trimming. The technique is based on careful calibration, and employs *e*-beam dose modulation to achieve relative dimensional control to below 1/50th of the SEBL address grid step size. We found stochastic variations to be important as they result in a standard deviation of the average ring waveguide width of 0.12 nm.

## ACKNOWLEDGMENTS

This work made use of MIT's shared scanning-electron-beam-lithography facility in the Research Laboratory of Electronics (SEBL at RLE). This research was supported by the DARPA EPIC Program under Contract No. W911NF-04-1-0431.

[1] T. Barwicz, M. A. Popovic, P. T. Rakich, M. R. Watts, H. A. Haus, E. P. Ippen, and H. I. Smith, Opt. Express **12**, 1437 (2004).
[2] T. Barwicz, Ph.D. thesis, MIT, 2005.
[3] F. X. Kärtner *et al.*, Proc. SPIE **6125**, 16 (2006).
[4] M. A. Popovic, C. Manolatau, and H. A. Haus, Opt. Express **14**, 1208 (2006).
[5] T. Barwicz, M. A. Popovic, M. R. Watts, P. T. Rakich, E. P. Ippen, and H. I. Smith, J. Lightwave Technol. **24**, 2207 (2006).
[6] J. G. Goodberlet, J. T. Hastings, and H. I. Smith, J. Vac. Sci. Technol. B **19**, 2499 (2001).
[7] T. Barwicz, M. A. Popovic, P. T. Rakich, M. R. Watts, H. A. Haus, E. I. Ippen, and H. I. Smith, Opt. Express **12**, 1437 (2004).